A cadaveric validation of a method based on impact analysis to monitor the femoral stem insertion

Arnaud Dubory, Giuseppe Rosi, Antoine Tijou, Hugues Albini Lomami, Charles-Henri Flouzat-Lachaniette, Guillaume Haïat

A cadaveric validation of a method based on impact analysis to monitor the femoral stem insertion

Arnaud Dubory[a,c], Giuseppe Rosi[b], Antoine Tijou[b], Hugues Albini Lomami[c], Charles-Henri Flouzat-Lachaniette[a], Guillaume Haiat[b]

[a]Service de Chirurgie Orthopédique et Traumatologique, Hôpital Henri Mondor AP-HP, CHU Paris 12, Université Paris-Est, 51 avenue du Maréchal de Lattre de Tassigny, 94000 Créteil, France.
[b]CNRS, Laboratoire de Modélisation et de Simulation Multi-Echelle, UMR CNRS 8208,61 Avenue du Général de Gaulle, Créteil 94010, France
[c]INSERM U955, IMRB Université Paris-Est, 51 avenue du Maréchal de Lattre de Tassigny, 94000 Créteil, France.

Corresponding author:
Guillaume Haiat
Laboratoire de Modélisation et de Simulation Multi Echelle, UMR CNRS 8208,
61 avenue du Général de Gaulle,
94010 Créteil, France
tel : (33) 1 45 17 14 41
fax : (33) 1 45 17 14 33
e-mail : guillaume.haiat@univ-paris-est.fr

Submitted to JMBBM.

Abstract

The success of cementless hip arthroplasty depends on the primary stability of the femoral stem (FS). It remains difficult to assess the optimal impaction energy to guarantee the FS stability while avoiding bone fracture. The aim of this study is to compare the results of a method based on the use of an instrumented hammer to determine the insertion endpoint of cementless FS in a cadaveric model with two other methods using i) the surgeon proprioception and ii) video motion tracking.

Different FS were impacted in nine human cadaveric femurs. For each configuration, the number of impacts realized when the surgeon felt that the FS was correctly inserted was noted N_{surg}. For each impact, the insertion depth E was measured and an indicator D was determined based on the time-variation of the force. The impact number N_{vid} (respectively N_d), corresponding to the end of the migration phase, was estimated analyzing the evolution of E (respectively D).

The respective difference between N_{surg}, N_{vid} and N_d was similar and lower than 3 for more than 85% of the configurations.

The results allow a validation of the use of an impact hammer to assess the moment when the surgeon should stop the impaction, paving the way towards the development of a decision support system to assist the surgeon.

Keywords

Hip arthroplasty; Cementless femoral stem; Primary stability; Impact analysis

Introduction

Total hip cementless arthroplasty is more and more often used in clinical practice (Yu et al., 2016). The femoral stem (FS) is impacted using a hammer within the femur that had previously been reamed. The pre-stressed state of the bone-implant system allows to obtain the primary stability of the FS, which is determinant for the short and long term surgical success. Despite a routine clinical use, there remain risks of failure, which may be due to i) peri-prosthetic femoral fracture, in particular because of FS oversizing (Sidler-Maier and Waddell, 2015) (with an incidence of 0.1-27.8% for intra-operative fractures and 0.07-18% for post-operative fracture) and ii) FS sinking into the femoral shaft, in particular in the case of FS undersizing. Both situations lead to FS aseptic loosening (Havelin et al., 2009; Hengsberger et al., 2001; Hoc et al., 2006) (with an incidence of 2.1 – 10.2%), which is due to micromotion at the bone-implant interface (Gheduzzi and Miles, 2007).

In order to decrease the risks of surgical failure, a compromise must be found by the surgeon in a patient specific manner regarding i) the number and the energy of the impacts realized when inserting the femoral stem in the femur, ii) the size of the chosen FS and iii) the depression of the FS into the femoral shaft. The perfect determination of the insertion endpoint corresponding to optimal contact conditions between the femoral cortical bone and the FS is essential. The number and the energy of the impacts should be sufficiently large in order to obtain a good primary stability of the FS and thus to avoid risks of migration; but should remain sufficiently low to avoid risks of intra-operative and post-operative peri-prosthetic fracture. In order to reach the aforementioned compromise, surgeons use empirical methods in clinical practice such as their proprioception, in particular by listening to the acoustic signature of the impacts between the hammer and the ancillary (Morohashi et al., 2017; Whitwell et al., 2013). Note that some authors have also monitored periprosthetic fractures of femora by measuring the femoral strain at the time of implantation (Schwarz et al., 2018).

Recently, an approach aiming at assessing the hip implant primary stability was developed by our group. This technique is based on the analysis of the time dependence of the force applied to the ancillary (that was retrieved using a piezo-electric sensor) during the impacts. The first studies focused on the acetabular cup (AC) implant and considered reproducible mass drops, which allowed to show that it was possible to monitor the AC implant insertion in bovine bone samples by analyzing the behavior of the contact duration (Mathieu et al., 2013; Michel et al., 2014). Another indicator based on the impact momentum was developed and was shown to be more accurate to assess the AC implant primary stability (Michel et al., 2015). Based on these results, the piezoelectric force sensor was screwed on the impacting face of a hammer and the technique was adapted to predict the AC implant stability *in vitro* (Michel et al., 2016b). An alternative hammer instrumented by strain sensors was also developed to assess the AC

implant stability (Tijou et al., 2017). In order to understand the phenomena occurring during the AC insertion, static (Nguyen et al., 2017a) and dynamic (Michel et al., 2017) finite element models have been developed. Eventually, a cadaveric study has been conducted using the aforementioned instrumented hammer and showed that it could be used in situations closed to those met in the operating room in order to estimate the AC implant primary stability (Michel et al., 2016a). The technique using the same instrumented hammer was then applied to study the insertion of the FS in bone mimicking phantoms (Tijou et al., 2018). An indicator based on the time of the second local maximum of the variation of the force as a function of time (which was determined using the force sensor) was used to estimate the insertion endpoint of the FS. However, the experiments were realized with bone mimicking phantoms held in a rigid frame and the application of such approach in a situation comparable to those met in the operating room has not been described, which would be of interest in the context of the development of a decision support system that could eventually be used in clinical practice. Recently, Oberst et al (Oberst et al., 2018) have used an impact hammer in combination with a regularization technique in cadaver experiments, leading to promising results but the method was not used to follow the insertion of a FS into the femoral shaft.

The aim of this study is to compare the results of a method based on the use of an instrumented hammer to determine the insertion endpoint of cementless FS in a cadaveric model with two other methods using i) the surgeon proprioception and ii) video motion tracking. To do so, the instrumented hammer has been used to insert different FS in nine human cadavers. The instrumented hammer was employed throughout the impaction procedure in order to estimate the variation of the signal as a function of the impact number. An optical system was used to follow the insertion of the FS using video motion tracking (VMT) techniques. The orthopedic surgeon was asked to determine, based on his proprioception, when he empirically felt that the stem was fully inserted.

Materials and methods

Implants, ancillaries and specimens

The cementless FS used (CERAFIT R-MIS) were manufactured by Ceraver (Roissy, France). Seven sizes were used (from size 7 to 13). All FS were made of titanium alloy (TiAl6V4) with a rough hydroxyapatite coating (the precise roughness was not provided by the manufacturer). The FS is equipped of 2 fins on each size to block the rotational movement of FS in the femoral shaft. Corresponding rasps and ancillaries were also provided by Ceraver (Roissy, France). Raps allow compacting the cancellous femoral bone in order to create a space into the femoral shaft and to embed the FS with an equivalent size. During the insertion of the FS, a home-made ancillary was screwed directly within the FS in order to obtain a rigid bilateral fixation between the FS and the ancillary, as shown in Fig. 1.

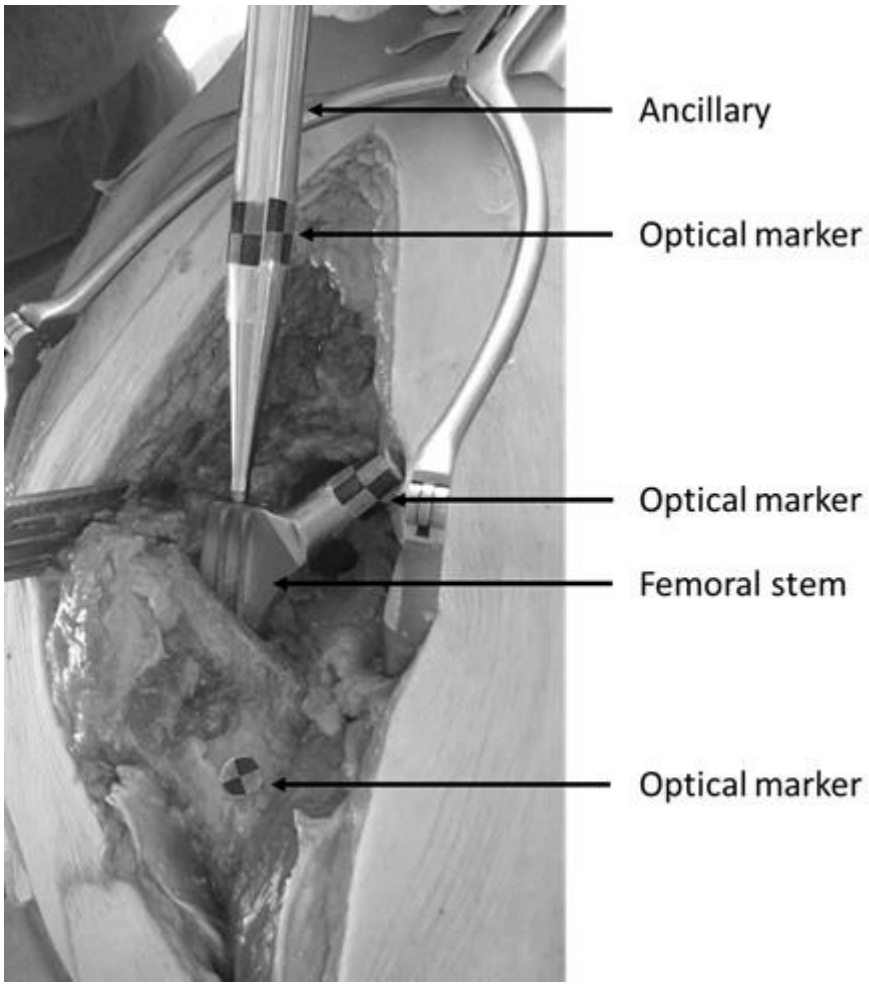

Figure 1. Image of the femoral stem being inserted into the femoral bone.

Nine cadavers were used in this study. All experiments were conducted in the Surgery School of the Fer à Moulin (Paris, France), a French institution providing cadavers and operating facilities for research and education purposes. Patient data were not available to authors. The ethical committee approved this study and did not ask any consent of the next of kin. Both femurs of each cadaver were tested as many times as possible in order to achieve an optimal use of the cadavers, which was required by the ethical committee. However, no FS could be inserted into four femurs because of various pathologies such as bone tumors, femoral fractures or trabecular calcification. Therefore, the FS were inserted into a total of 14 femurs.

All femoral bones were prepared following the same protocol. The cadavers were placed in lateral decubitus position. A large incision was realized using a posterior approach (Moore) in order to obtain an unobstructed view of the femur distal part as shown in Fig.1. Then, the femoral head was dislocated. Finally, the osteotomy of the femoral neck was performed following the usual clinical protocol. All experiments were carried out by three experienced orthopedic surgeons.

Instrumented hammer

The hammer (m=1.3 kg) used to insert the FS was the same as the one used in several previous studies focusing on the AC implant (Bosc et al., 2018; Michel et al., 2016a; Michel et al., 2016b) and the femoral stem (Tijou et al., 2018) insertion. A dynamic piezoelectric force sensor (208C05, PCB Piezoelectronics, Depew, New York, USA) was screwed to the center of the impacting face of the hammer. All impacts were realized directly on the force sensor so that the variation *s(t)* of the force as a function of time could be measured.

Femoral stem insertion and signal processing

Each impact was performed using the instrumented hammer described above. A data acquisition module (NI9234, National Instruments, Austin, TX, USA) with a sampling rate of 51.2 kHz and a resolution of 24 bits was used to record the time-variation of the force *s(t)* applied between the hammer and the ancillary. The data were then transferred to a computer and recorded using a Labview interface (National instruments, Austin, TX, USA) for a duration of 7 ms.

A dedicated signal processing technique was developed in order to extract information from each signal *s(t)* corresponding to each impact. The beginning of the impact (*t*=0) was defined when the signal first exceeded a threshold of 200 N using a dedicated trigger. The time difference (noted *D* in what follows) between the time of the second and the first local maxima of *s(t)* was determined following:

$$D = t\left(\left[\max 2\ s(t)\right]\right) - t\left(\left[\max 1\, s(t)\right]\right) \qquad (1)$$

where the function *max1* denotes the time of the maximum value of the signal, named first peak, and the function *max2* denotes the time of the second local maximum, named second peak, for which the following conditions are fulfilled. First, the prominence of the peak, noted α, and representing the difference between the maximum amplitudes of the peak and of the closest local minimum, must be higher than 100 N. Second, the time difference between the first peak defined above and that of the considered peak, called β, must be higher than 0.3 ms. Third, the parameter γ, representing the width of the peak at the half of the prominence α, must be higher than 0.04 ms. The choice of the parameters α, β and γ will be analyzed in the discussion section.

Video motion tracking

In order to measure the relative displacement of the FS compared to the femoral shaft, a camera (Powershot SX410 IS, Canon, Tokyo, Japan) with a frame rate of 24 frames per second and a high-definition resolution of 1280x720 pixels was used to record the displacement of the bone-implant system throughout the impaction procedure. Optical markers were placed on the FS implant, on the ancillary

and on the femur (see Fig. 1). The relative displacements of the markers after each impact were determined using the software Tracker (Cabrillo College, Aptos, CA, USA).

The indicator *E* corresponding to the relative displacement of the FS compared to the femoral bone was obtained by analyzing the video and was defined as:

$$E(i) = d(0) - d(i) \quad (2)$$

where *d(i)* corresponds to the distance between the markers located on the femoral bone and on the ancillary after the i^{th} impact and *d(0)* corresponds to the initial distance between these both markers. Note that the increment *i* is defined relatively to the beginning of the impaction procedure. The distance between the two optical markers on the FS and on the ancillary was constant during the experiment and was used to convert pixels into centimeters.

Experimental protocol

Figure 2 summarizes the experimental protocol carried out by trained orthopedic surgeons for each femur and described in more details in what follows.

The surgeon determined empirically the size of the FS that would have been chosen in clinical practice. A cavity was initially created in each femur using the rasp corresponding of the chosen FS. Then, the following impaction procedure was carried out, which consists in two consecutive steps. Firstly, the surgeon inserted the FS corresponding to the size of the rasp using the instrumented impact hammer until he empirically considered that an optimal stability condition was obtained. The number of impacts needed to obtain this "optimal" stability condition was noted N_{surg}. Secondly, twelve additional impacts with a first peak amplitude varying between 1 and 14 kN were performed in order to determine whether the FS could be further inserted. The choice of the values used for the first peak amplitude (between 1 and 14 kN) and for the number of additional impacts (12) will be analyzed in the discussion section. For each impact, the values of the indicators *D* and *E* were determined following the two protocols described above.

The impaction procedure was repeated as many times as possible (*i.e.* as long as the femur was not fractured, which was checked visually) in order to maximize the number of configurations, which was requested by the ethical committee. As shown in Fig. 2, the FS was extracted from the femur at the end of each impaction procedure and the surgeon checked if the femur was fractured. If so, the protocol was ended. If not, the surgeon reproduced the same impaction procedure as long as the femur macroscopic status allowed to do so, which was checked using a template of the FS of the same size. When the surgeon considered that realizing an impaction procedure using the same implant was no longer possible because the FS became undersized due to the modification of bone structure (in particular bone compaction and removal (Husseini et al., 2018)) related to multiple insertion of the FS, the surgeon determined if it was possible to use a larger implant size. If so, the protocol was carried on using a larger rasp and implant size. If not, the protocol was ended. Note that the rasp used for uncemented FS allows

to obtain a cavity located inside the femoral shaft by both removing and compacting cancellous bone in order to obtain a good geometrical fit between the FS and the remaining bone (Husseini et al., 2018). The rasp creates a cavity into femoral bone explaining that for a same femoral shaft, several sizes may be adapted according to the size of the last rasp employed. The geometrical congruence between the FS and the femoral shaft corresponds to the endpoint for which the FS does not create a femoral fracture during its insertion (oversized FS) and does not progressively move into the femoral shaft (undersized FS). Note that since the appropriate rasp (corresponding to the inserted FS) was used at the end of the reaming process and before the FS insertion, the size of the cavity is likely to correspond to that of the FS, except when the FS is varus positioned (see discussion section). The good fit between the cavity and the FS is obtained through the conception of the rasp and of the FS by the implant manufacturer.

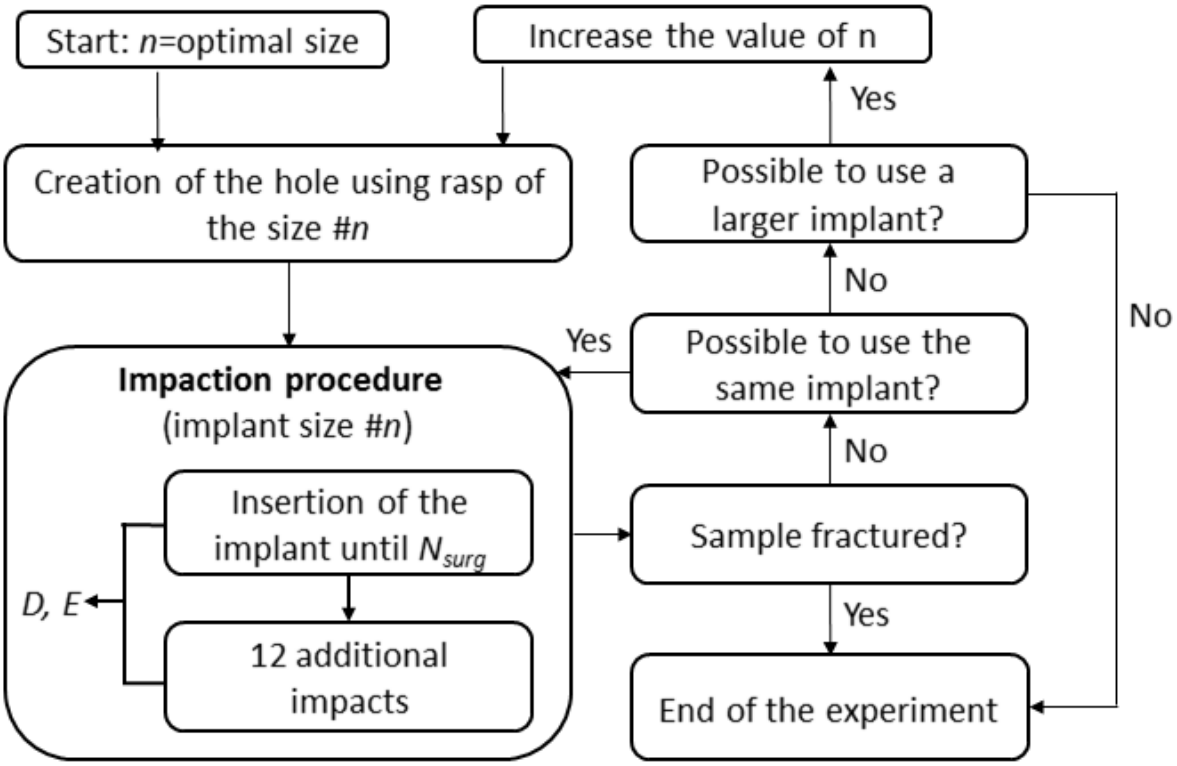

Figure 2. Schematic representation of the experimental protocol realized for each femoral bone sample.

Post-processing and data analysis

Following the experimental protocol described above, three different methods were employed for each impaction procedure in order to estimate the number of impact necessary to "fully" insert the FS within the femur. This "full" insertion thus corresponds to an estimation of the end of the migration phase of the FS in the femur.

The first method consists in analyzing the variation of *D(i)*, which corresponds to the time difference between the first and second maxima as a function of the impact number *i*. For each impaction

procedure, the parameter N_d was defined as the number of the second consecutive impact satisfying(Tijou et al., 2018):

$$D(i) \leq D_{th}, \qquad (3)$$

where D_{th} is a threshold chosen equal to 0.57 ms. The choice of this value will be analysed in the discussion section.

The second method consists in analyzing the variation of the parameter *E(i)* corresponding to the position of the FS relatively to the femoral bone as a function of the impact number *i*. For each impaction procedure, the parameter N_{vid} was defined as the number of the first impact that satisfies the following inequality (Tijou et al., 2018):

$$E(i) \geq E_m - \delta * E_{sd} \qquad (4)$$

where E_m and E_{sd} are respectively the average and standard deviation of the values of *E* obtained for the last eleven impacts and δ is a parameter empirically chosen equal to 2.2. The choice of the value of the parameter δ*=2.2* will be described in the discussion section. Note that the insertion endpoint, defined by $E_{th} = E_m - \delta * E_{sd}$ in Eq. 4, depends on the impaction procedure.

Eventually, the third method consists in using the proprioception (touch, sight and hearing) of the surgeon, similarly as what is done in clinical practice, to determine when he felt that the FS was totally inserted, leading to the parameter N_{surg}.

The differences between the values found for N_{surg}, N_d and N_{vid} were determined for each impaction procedure. Namely, the difference between N_{surg} and N_d (respectively (N_{surg} and N_{vid}) and (N_d and N_{vid}) is denoted M_d (respectively M_{vid} and M_c) following:

$$M_d = N_d - N_{surg}\,, \quad M_{vid} = N_{vid} - N_{surg}\,, \quad M_c = N_{vid} - N_d\,. \qquad (5)$$

The average and standard deviation values of M_d, M_{vid} and M_c were determined over all configurations as well as the percentage of cases where M_d, M_{vid} and M_c were comprised between -3 and +3.

Results

Table 1 shows the number of impaction procedures considered for each cadaver. The total number of configurations was equal to 77.

Figure 3 shows two signals *s(t)* corresponding to the fourteenth and the twenty-second impact obtained for a given configuration (subject #7, right femur, implant size = 12 and test #1). Figure 3 illustrates the method used to determine the value of *D* for each impact. The vertical solid black line corresponds to the time of the first peak. The time difference between the time of the first peak and the vertical black

dotted line corresponds to the threshold D_{th} = 0.57 ms. The dashed vertical grey (respectively black) line represents the time of the second peak of the fourteenth (respectively twenty-second) impact.

	Femur number									
Size of implant	#1	#2	#3	#4	#5	#6	#7	#8	#9	Total
7	2							3		**5**
8	3				2			1		**6**
9					3	1				**4**
10	2		2	2	7	4	2		6	**25**
11	3	1	1			5	4		5	**19**
12	1	3				4	5			**13**
13		4							1	**5**
Total	**11**	**8**	**3**	**2**	**12**	**14**	**11**	**4**	**12**	**77**

Table 1. Number of configurations considered for each FS implant size and each femur, leading to a total number of 77 configurations considered in this study.

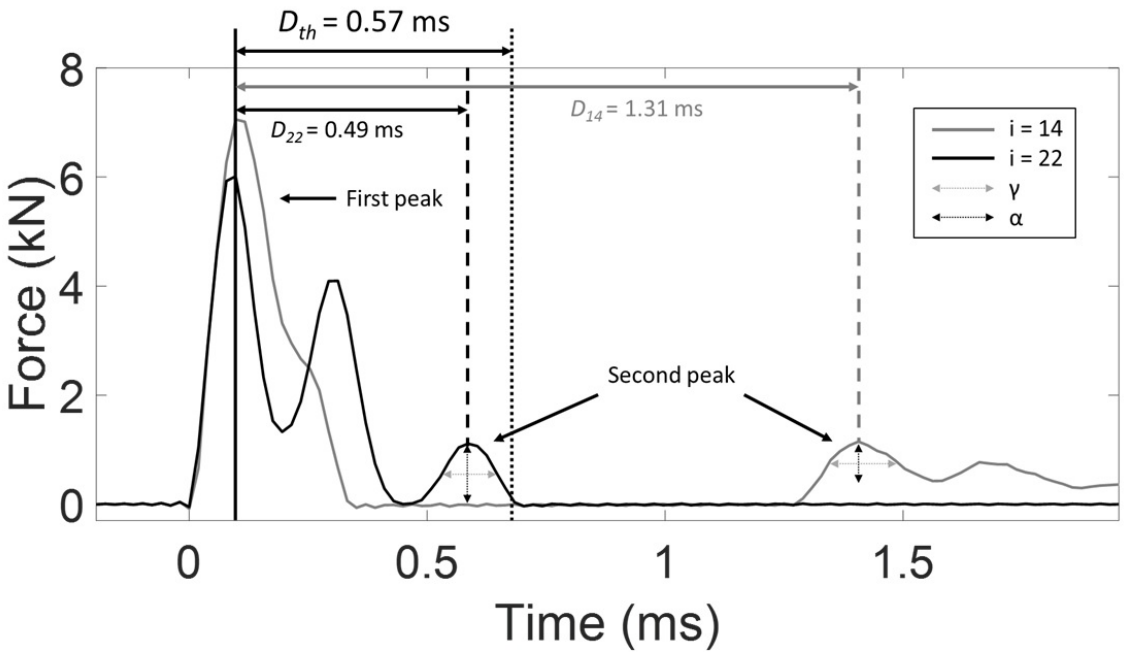

Figure 3. Two signals corresponding to the time variation of the force obtained during impacts of the instrumented hammer on the ancillary linked to the femoral stem for a given impaction procedure (subject #7, right femur, size of implant 12, test #1). *i* indicates the impact number (*i*=1 corresponding to the beginning of the impaction procedure). The first and second peak are indicated by solid and dashed vertical lines respectively. The parameters α and γ are shown for both second peaks. The values of D_{14}, D_{22} and of the threshold D_{th} are also shown.

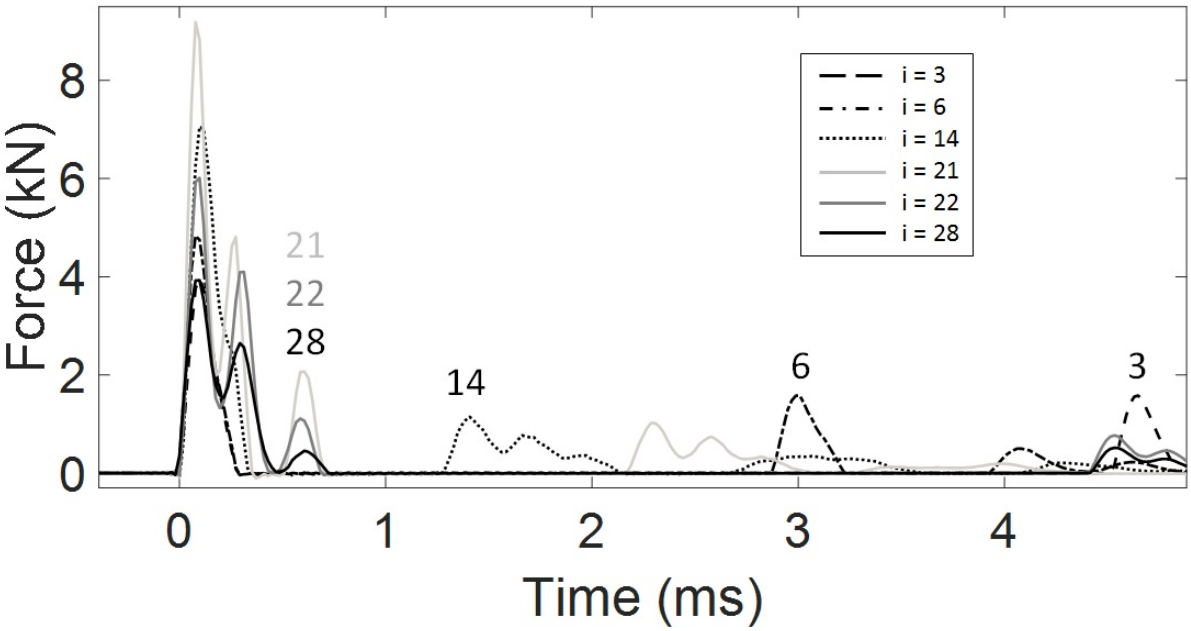

Figure 4. Six signals corresponding to the time variation of the force obtained during impacts of the instrumented hammer on the ancillary linked to the femoral stem for the same impaction procedure as the one shown in Fig. 3. *i* indicates the impact number (*i*=1 corresponding to the beginning of the impaction procedure).

Figure 4 shows six examples of force signals *s(t)* obtained for the same configuration as the one used in Fig. 3, which were chosen arbitrarily for illustration purposes. The respective number of each impact is indicated above each corresponding second peak of the signal. The signals shown correspond to the third, sixth, fourteenth, twenty-first, twenty-second and twenty-eighth impact. As illustrated in Fig. 4, the time of the second peak first decreases and then stays constant after the twenty-first impact.

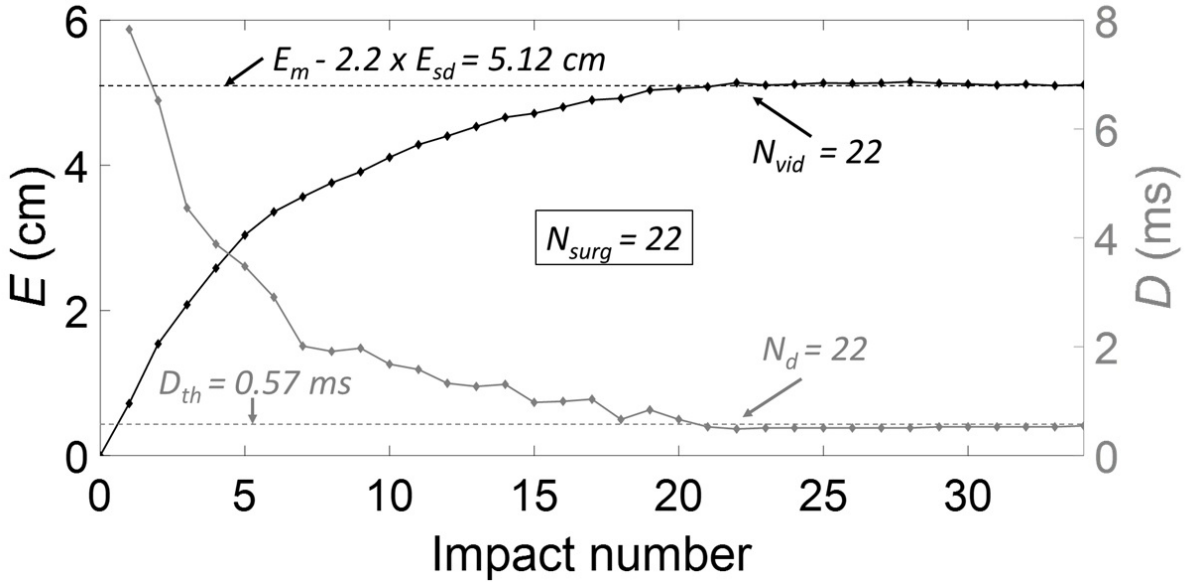

Figure 5. Variation of the parameters *D* (grey line) and *E* (black line) corresponding respectively to the time difference between the first and second peaks and to the implant penetration depth as a function of the impact number for the same configuration as the one corresponding to Figs. 3&4. The horizontal dashed black line represents the penetration equal to $E_m - \delta$ x E_{sd} and the horizontal dotted black line represents the threshold D_{th} = 0.57 ms.

Figure 5 shows the variation of the parameters *D* and *E* as a function of the impact number *i* for the same configuration as the one corresponding to Figs. 3&4. The reference value given by the surgeon, namely N_{surg} is equal to 22. The horizontal dashed black (respectively grey) line represents the penetration equal to $E_m - \delta$ x E_{sd} (respectively the threshold D_{th} = 0.57 ms). For this configuration $N_{surg} = N_d = N_{vid} = 22$, which leads to $M_d = M_{vid} = M_c = 0$.

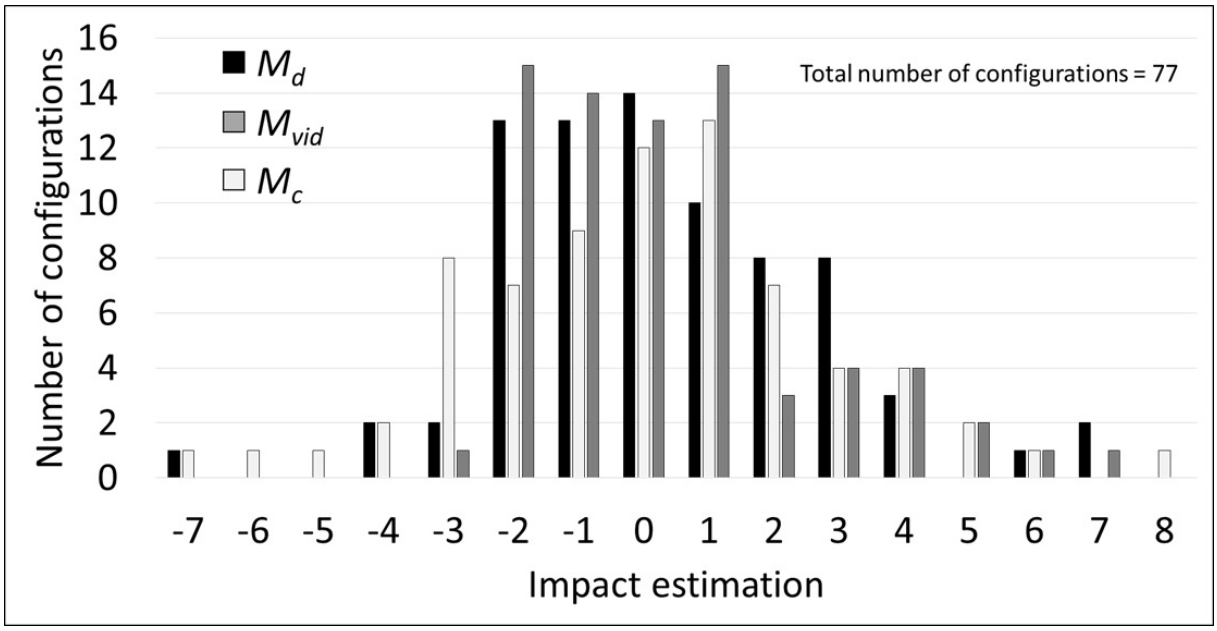

Figure 6. Distribution of the values obtained for M_d, M_{vid} and M_c.

Figure 6 shows the distributions of the results obtained for M_d, M_{vid} and M_c, which corresponds to the difference obtained between the three different methods for the estimation of the insertion endpoint of the FS in the sample. Table 2 shows the average and standard deviation values of M_d, M_{vid} and M_c as well as the percentage of configurations for which the values of M_d, M_{vid} and M_c are comprised between -3 and +3.

	Average	Standard deviation	% between -3 and +3
M_d	0,29	2,44	88
M_{vid}	0,34	2,16	89
M_c	0,08	2,74	82

Table 2. Average values, standard deviation values and percentage of M_d, M_{vid} and M_c between -3 and +3.

Discussion

The originality of the present study is to show the feasibility of extracting information from the time dependence of the force applied to the ancillary during impacts in order to follow the insertion of the femoral stem within cadaveric femurs. The method is based on the analysis of the time-variation of the force transmitted between the hammer and the ancillary during the impact and measured using a dedicated instrumented hammer.

The aim of the present study was similar to the aim of (Morohashi et al., 2017) who used a microphone to record the sound produced by the impact in order to assess the insertion endpoint of the FS. However, in the present study, the sensor is positioned directly at the impacting surface, which allows to record vibrations directly where it is generated, while recording the sound produced by the impact at a distance is likely to lead to loss of information. A careful comparison of the two techniques would be of interest to complement both approaches. Note that the use of video motion tracking would not be easy in clinical practice due to the difficulty of obtaining a stable video of the insertion in the operating room.

The number of impacts required to obtain a "full" insertion of the FS in a cadaveric femur is assessed with three methods using i) video motion tracking, ii) the proprioception of the surgeon and iii) the instrumented hammer. The results show a good agreement between the three methods, which constitutes a validation of our approach. However, there remain errors between the results obtained with the three methods (see Fig. 6 and Table 2), which can be explained by the following factors. First, the proprioception of the experienced surgeons who carried out the experiments was considered (leading to the estimate N_{surg}), similarly as what is done in clinical practice. The surgeon's feeling is based on tactile sensations, hearing and vision. Although informative, this method has the drawback of depending on the surgeon and to be associated to possible bias, which were estimated by the surgeon of around ± 3. Second, the VMT based method also suffers from errors, which are due i) to changes of angular position, ii) possible macroscopic 3-D movements and plastic bone deformation and iii) errors based on the image processing technique. Therefore, the aforementioned factors lead to an error on N_{vid} equal to around ± 3. The difference obtained between the three techniques shown in Fig. 6 and Table 2 are of the order to magnitude of the cumulative errors described above. Note that the error obtained between N_{surg} and N_{vid}, which does not depend the impact hammer, is of the same order of magnitude than the errors obtained between i) N_{surg} and N_d and ii) N_d and N_{vid}.

Figures 3, 4 and 5 show that the value of the indicator D, which corresponds to the time of the second peak of the signal decreases as a function of the number of impacts. When the FS is inserted into the host bone, the bone-implant contact ratio increases, which leads to an increase of the overall rigidity of the bone-implant system. Note that the increase of the rigidity of the system may in turn explain the increase of its resonance frequency, which leads to a decrease of the difference between the first and second peak of the signal. The increase of the resonance frequency corresponding to an increase of the

bone-implant contact ratio has already been evidenced analytically (Michel et al., 2014) and numerically (Michel et al., 2017). Note that the increase of the resonance frequency during the insertion is in qualitative agreement with the results found by Oberst et al. (Oberst et al., 2018) using a comparable approach.

In this study, several parameters were chosen empirically. First, the choice of the number of additional impacts given by the surgeon after N_{surg} (equal to twelve) was the result of a compromise between i) a sufficiently high number to obtain a convergence for the variation of the indicators D and E and ii) a sufficiently low number to minimize fracture risks.

Second, the upper bound of the range of variation of the maximal force [1– 14 kN] of the last eleven impacts realized once the surgeon felt that the FS is fully inserted (i.e. after N_{surg}) was chosen sufficiently low in order to minimize fracture risk. The range of variation (13 kN) was chosen sufficiently wide in order to be able to determine the influence of the maximal force on the value of D. Note that this range of variation is similar to the typical range applied by the surgeon during the insertion, i.e. before N_{surg}.

Third, the choice of the value of D_{th} = 0.57 ms was made following the results shown in Fig. 7, which corresponds to the variation of the values of D obtained for the 847 (corresponding to 11*77) impacts realized after N_{surg} + 1 impact. The dotted line corresponds to the threshold equal to 0.57 ms chosen for D_{th}. As shown in Fig. 7, the value of D was higher than D_{th} for only 11 impacts out of 847 (i.e. 1.3 %), which constitutes a validation of the approach and explains the choice of D_{th}. Moreover, no significant variation of the value of D was obtained as a function of the amplitude of the first peak.

Fourth, the parameter δ (equal to 2.2) was chosen empirically to find a compromise between a sufficiently high value to account for the constant increase of E after N_{surg} and a sufficiently low value in order not to underestimate E_m. Varying the value of δ between 1.8 and 2.6 did not alter the value of N_{vid} (less than 10%, data not shown).

Fifth, the value of 200 N used for the threshold defining the beginning of the contact between the hammer and the ancillary was chosen to find a compromise between a sufficient value compared to the signal to noise ratio and a value small enough to provide a good accuracy of detection. Changing the value of the detection this threshold between 150 and 250 N did not modify the results.

Sixth, the parameters used to detect the second peak were chosen empirically. Variations of α between 50 N and 150 N, β between 0.25 ms and 0.35 ms and γ between 0.06 ms and 0.14 ms do not change the value of N_d (data not shown).

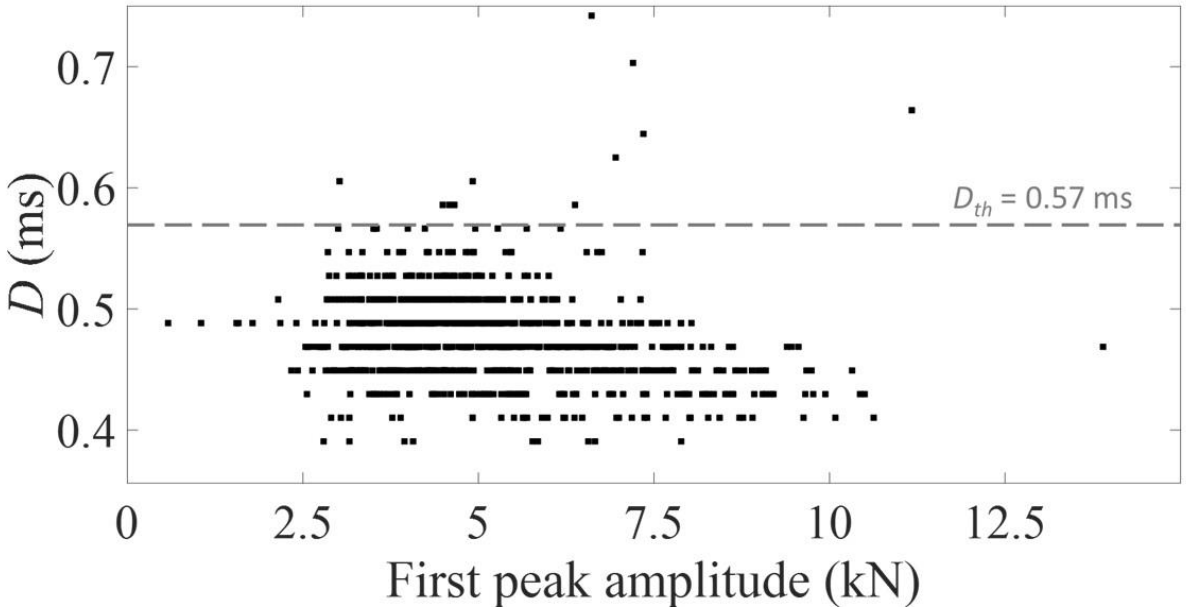

Figure 7. Variation of the time difference *D* between the first and second peaks of the signal for all impacts realized after N_{surg} +1 (i.e. when the femoral stem is fully inserted) impacts for all configurations as a function of the amplitude of the first peak. The horizontal dashed grey line represents the threshold D_{th} = 0.57 ms chosen to determine when the femoral stem is fully inserted (N_d).

A first limitation of the present study lies the use of human cadaveric femur. Living bone properties may differ from those of cadaveric bone. Another limitation lies in that a limited number of femurs were considered. In particular, D_{th} is a parameter set based on the results obtained with all 77 configurations corresponding to the 9 cadaveric femurs considered. The choice of the value of D_{th} = 0.57 ms was made based on the results shown in Fig. 7, which indicates that the value of *D* obtained for all impacts realized when the femoral stem is fully inserted (i.e. for $N > N_{surg} + 1$), was almost always lower than D_{th}. However, more samples should be considered in order to validate the choice made for the value of D_{th} and therefore to develop a more reliable decision support system. Moreover, each cadaveric femur was used many times, so their respective biomechanical response could vary. Reusing the samples results in each specimen being exposed to a different number of impacts that may in turn results in micro-level changes in the bones structure. Nevertheless, it would not be acceptable from an ethical point of view to use cadaveric human femurs just once and it was requested by the ethical committee to validate the technique in cadavers before testing our approach in patients Another limitation of this work is the lack of radioscopic control during the procedure (which could have been done following (Laine et al., 2001)) in order to check the direction of FS impaction into the femoral shaft and to verify the size of the FS according to the volume of the femoral shaft. Indeed, a varus or valgus the FS position could lead to an error on the endpoint estimation given by the impact analysis.

A second limitation lies in the fact that we did not analyze the occurrence of fracture during the FS insertion, which would require additional imaging modality that are not currently available. Instead, we

checked visually at the end of each experiment (see Fig. 2) whether the femur was fractured, which indicated the end of the experiment for the corresponding femur. It would be very useful to be able to tell the surgeon when the fracture actually occurs during impacts, which is difficult to assess during surgery. However, the present study does not deal with fracture detection, which is left to future studies. Instead, the aim of the study is to determine whether it is possible to use an instrumented hammer to retrieve information on the insertion endpoint of the FS and to relate this information to the same one obtained with two different modalities (i.e. the proprioception of the surgeon and the video motion tracking).

A third limitation comes from the fact that the present analysis only applies to CERAFIT R-MIS FS implant and further work would be necessary to adapt the method to different FS implants.

A fourth limitation comes from the fact that different sizes of FS were used for each femur, which would not be the case in clinical practice. The normal procedure would be to perform preoperative templating and intraoperative fluoroscopy of the rasp before implantation of the FS. Note that we choose to adopt the experimental protocol described in Fig. 2 in order to make good use of the anatomical subjects, as requested by the ethical committee. Here, we analyzed the insertion endpoint of the FS for various sizes of FS and cavity. However, for each configuration, the femur was reamed using rasps corresponding to the tested FS, which limits the possibility of obtaining severely undersized or oversized FS compared to the cavity. Moreover, the surgeons verified that for all configurations, the FS was stable and correctly seated in the femur. If it was not the case, the femur was reamed to achieve a good positioning of the FS in the femur. Note that a very similar protocol was used in our previous paper concerning the acetabular cup implant (Michel et al., 2016a). Despite this assumption, it was always possible to use the instrumented hammer in an effective manner. Considering slightly undersized or oversized FS does not lead to optimal primary stability conditions. However, primary stability is not assessed in the present study and this point was studied in (Tijou et al., 2018) in the case of FS inserted in bone mimicking phantoms. The surgeon checked manually that the FS was stable at the end of the insertion for all configurations. We could not measure the pull-out force in the present study because the primary stability was so important that the pull-out force could not be assessed using a manual dynamometer. We choose not to use a testing machine due to the difficulty of bringing it to the surgery school where the samples were tested. Note that we choose to realize the experiments in using the entire body because considering isolated femurs (which would make the use of a testing machine possible) is likely to modify the results obtained with the instrumented hammer. Therefore, investigating the FS stability is considered to be out of scope of the present study, which only focuses on the insertion endpoint that may be reached independently of the FS size. Using radiographic analysis at the end of each insertion could provide valuable information on the FS seating (in particular using the approach described in (Laine et al., 2001)) and such approach should be used in future studies. However, radiographic analyses are not likely to provide information on the amount of bone in contact with the implant. Moreover, if the FS or the rasp is not accurately positioned within the femoral shaft, the FS may be inserted in varus,

leading to a contact between the FS and bone tissue occurring mainly in the external layer of cortical bone. The case of a varus positioned FS is possible and may not be detected neither by the surgeons (who may have the same proprioception), nor by the instrumented hammer. This point should be considered in future studies.

A fifth limitation is associated to the fact that bone density was not measured and future studies will focus on the relation between the signal and bone quality. The aim of this study was to show that using an instrumented hammer was possible independently of the bone density which is not always measured preoperatively. Moreover, in the present study, we could not use an x-rays template or a digital template because we did not have preoperative pelvic ring x-rays. Instead, the size of the FS used initially has been empirically determined according to the surgeon experience. Similarly, we did not carry out intraoperative fluoroscopy in order to evaluate the radiologic contact between cortical bone and the FS and to verify the absence of varus position into the femoral shaft, which is left to future studies.

Conclusion

This study shows that the analysis of the time variation of the force between the hammer and the ancillary during the insertion of the femoral stem allows to assess the moment when the FS is positioned under an acceptable press-fit condition into the host femoral bone. This approach could constitutes the basis for the development of a future medical device consisting in a real-time decision support system helping surgeons to adapt their surgical strategy in a patient specific manner. More specifically, an alert could be implemented and activated when the FS is expected to be fully inserted, thus avoiding unnecessary additional impacts which may lead to fracture risks. A significant advantage of the current method lies in that it can be used without changing the surgical protocol. Future step will consist in i) testing the application of the present approach to impacts made when inserting the rasp, which may help to indicate the correct size of the implant before insertion of FS, ii) testing the application of the present approach to impact made when inserting the rasp, which may help to indicate the correct size before insertion of FS and iii) obtaining an instrumented hammer that can be sterilized in order to determine its performances in the operative room. Moreover, finite element modeling would be of great help to better understand the phenomena occurring when impacting the femoral stem within the femur and to understand the effect of undersizing and oversizing the FS compared to the femoral bone. Note that such approach has already been carried out by our group in the context of the insertion of acetabular cup implants (Michel et al., 2016c; Nguyen et al., 2017b). Numerical modeling will lead to an optimization of the technique and to improvements in the performance of the method.

Acknowledgements

This work has received funding from the European Research Council (ERC) under the European Union's Horizon 2020 research and innovation program (grant agreement N° 682001, project ERC Consolidator Grant 2015 BoneImplant).
This work has been realized thanks to the support of l'Ecole de Chirurgie du Fer à Moulin (Paris, France).
This work has received funding from the CNRS through the PEPS INGENIERIE TRANSLATIONELLE EN SANTE 2017 project "HipImpact".

References

Bosc, R., Tijou, A., Rosi, G., Nguyen, V.H., Meningaud, J.P., Hernigou, P., Flouzat-Lachaniette, C.H., Haiat, G., 2018. Influence of soft tissue in the assessment of the primary fixation of acetabular cup implants using impact analyses. Clin Biomech (Bristol, Avon) 55, 7-13.

Gheduzzi, S., Miles, A.W., 2007. A review of pre-clinical testing of femoral stem subsidence and comparison with clinical data. Proceedings of the Institution of Mechanical Engineers. Part H, Journal of engineering in medicine 221, 39-46.

Havelin, L.I., Fenstad, A.M., Salomonsson, R., Mehnert, F., Furnes, O., Overgaard, S., Pedersen, A.B., Herberts, P., Karrholm, J., Garellick, G., 2009. The Nordic Arthroplasty Register Association: a unique collaboration between 3 national hip arthroplasty registries with 280,201 THRs. Acta orthopaedica 80, 393-401.

Hengsberger, S., Kulik, A., Zysset, P., 2001. A combined atomic force microscopy and nanoindentation technique to investigate the elastic properties of bone structural units. Eur Cell Mater 1, 12-17.

Hoc, T., Henry, L., Verdier, M., Aubry, D., Sedel, L., Meunier, A., 2006. Effect of microstructure on the mechanical properties of Haversian cortical bone. Bone 38, 466-474.

Husseini, A., Nooh, A., Tanzer, D., Smith, K., Tanzer, M., 2018. Washing the Femoral Canal Results in More Predictable Seating of a Short, Tapered Femoral Stem. J Arthroplasty 33, 3220-3225.

Laine, H.J., Pajamaki, K.J., Moilanen, T., Lehto, M.U., 2001. The femoral canal fill of two different cementless stem designs. The accuracy of radiographs compared to computed tomographic scanning. Int Orthop 25, 209-213.

Mathieu, V., Michel, A., Flouzat Lachaniette, C.H., Poignard, A., Hernigou, P., Allain, J., Haiat, G., 2013. Variation of the impact duration during the in vitro insertion of acetabular cup implants. Med Eng Phys 35, 1558-1563.

Michel, A., Bosc, R., Mathieu, V., Hernigou, P., Haiat, G., 2014. Monitoring the press-fit insertion of an acetabular cup by impact measurements: Influence of bone abrasion. Proc Inst Mech Eng H 228, 1027-1034.

Michel, A., Bosc, R., Meningaud, J.P., Hernigou, P., Haiat, G., 2016a. Assessing the Acetabular Cup Implant Primary Stability by Impact Analyses: A Cadaveric Study. PLoS One 11, e0166778.

Michel, A., Bosc, R., Sailhan, F., Vayron, R., Haiat, G., 2016b. Ex vivo estimation of cementless acetabular cup stability using an impact hammer. Med Eng Phys 38, 80-86.

Michel, A., Bosc, R., Vayron, R., Haiat, G., 2015. In vitro evaluation of the acetabular cup primary stability by impact analysis. Journal of biomechanical engineering 137.

Michel, A., Nguyen, V.H., Bosc, R., Vayron, R., Hernigou, P., Naili, S., Haiat, G., 2016c. Finite element model of the impaction of a press-fitted acetabular cup. Med Biol Eng Comput.

Michel, A., Nguyen, V.H., Bosc, R., Vayron, R., Hernigou, P., Naili, S., Haiat, G., 2017. Finite element model of the impaction of a press-fitted acetabular cup. Med Biol Eng Comput 55, 781-791.

Morohashi, I., Iwase, H., Kanda, A., Sato, T., Homma, Y., Mogami, A., Obayashi, O., Kaneko, K., 2017. Acoustic pattern evaluation during cementless hip arthroplasty surgery may be a new method for predicting complications. SICOT J 3, 13.

Nguyen, V.H., Rosi, G., Naili, S., Michel, A., Raffa, M.L., Bosc, R., Meningaud, J.P., Chappard, C., Takano, N., Haiat, G., 2017a. Influence of anisotropic bone properties on the biomechanical behavior of the acetabular cup implant: a multiscale finite element study. Computer methods in biomechanics and biomedical engineering, 1-14.

Nguyen, V.H., Rosi, G., Naili, S., Michel, A., Raffa, M.L., Bosc, R., Meningaud, J.P., Chappard, C., Takano, N., Haiat, G., 2017b. Influence of anisotropic bone properties on the biomechanical behavior of the acetabular cup implant: a multiscale finite element study. Comput Methods Biomech Biomed Engin 20, 1312-1325.

Oberst, S., Baetz, J., Campbell, G., Lampe, F., Lai, J., Hoffmann, N., Morlock, M., 2018. Vibro-acoustic and nonlinear analysis of cadavric femoral bone impaction in cavity preparations. MATEC Web Conf 148, 14007.

Schwarz, E., Reinisch, G., Brandauer, A., Aharinejad, S., Scharf, W., Trieb, K., 2018. Load transfer and periprosthetic fractures after total hip arthoplasty: Comparison of periprosthetic fractures of femora implanted with cementless distal-load or proximal-load femoral components and measurement of the femoral strain at the time of implantation. Clin Biomech (Bristol, Avon) 54, 137-142.

Sidler-Maier, C.C., Waddell, J.P., 2015. Incidence and predisposing factors of periprosthetic proximal femoral fractures: a literature review. International orthopaedics 39, 1673-1682.

Tijou, A., Rosi, G., Hernigou, P., Flouzat-Lachaniette, C.H., Haiat, G., 2017. Ex Vivo Evaluation of Cementless Acetabular Cup Stability Using Impact Analyses with a Hammer Instrumented with Strain Sensors. Sensors (Basel) 18.

Tijou, A., Rosi, G., Vayron, R., H, A.-L., P, H., Flouzat Lachaniette, C., Haiat, G., 2018. Monitoring cementless femoral stem insertion by impact analyses: an in vitro study. J. Mech. Behav. Biomed. Mater 88, 102-108.

Whitwell, G., Brockett, C.L., Young, S., Stone, M., Stewart, T.D., 2013. Spectral analysis of the sound produced during femoral broaching and implant insertion in uncemented total hip arthroplasty. Proceedings of the Institution of Mechanical Engineers. Part H, Journal of engineering in medicine 227, 175-180.

Yu, H., Liu, H., Jia, M., Hu, Y., Zhang, Y., 2016. A comparison of a short versus a conventional femoral cementless stem in total hip arthroplasty in patients 70 years and older. Journal of orthopaedic surgery and research 11, 33.

Figures and tables

Figure 1. Image of the femoral stem being inserted into the femoral bone.

Figure 2. Schematic representation of the experimental protocol realized for each femoral bone sample.

Figure 3. Two signals corresponding to the time variation of the force obtained during impacts of the instrumented hammer on the ancillary linked to the femoral stem for a given impaction procedure (subject #7, right femur, size of implant 12, test #1). i indicates the impact number (i=1 corresponding to the beginning of the impaction procedure). The first and second peak are indicated by solid and dashed vertical lines respectively. The parameters α and γ are shown for both second peaks. The values of D_{14}, D_{22} and of the threshold D_{th} are also shown.

Figure 4. Six signals corresponding to the time variation of the force obtained during impacts of the instrumented hammer on the ancillary linked to the femoral stem for the same impaction procedure as

the one shown in Fig. 3. *i* indicates the impact number (*i*=1 corresponding to the beginning of the impaction procedure).

Figure 5. Variation of parameters *D* (grey line) and *E* (black line) corresponding respectively to the time difference between the first and second peaks and to the implant penetration depth as a function of the impact number for the same configuration as the one corresponding to Figs. 3&4. The horizontal dashed black line represents the penetration equal to $E_m - \delta$ x E_{sd} and the horizontal dotted black line represents the threshold D_{th} = 0.57 ms.

Figure 6. Distribution of the values obtained for M_d, M_{vid} and M_c.

Figure 7. Variation of the time difference *D* between the first and second peaks of the signal for all impacts realized after N_{surg} +1 (i.e. when the femoral stem is fully inserted) impacts for all configurations as a function of the amplitude of the first peak. The horizontal dashed grey line represents the threshold D_{th} = 0.57 ms chosen to determine when the femoral stem is fully inserted (N_d).

Table 1. Number of configurations considered for each FS implant size and each subject, leading to a total number of 77 configurations considered in this study.

Table 2. Average values, standard deviation values and percentage of M_d, M_{vid} and M_c between -3 and +3.